Diverse maize hybrids are structurally inefficient at resisting wind induced bending forces that cause stalk lodging

Christopher J. Stubbs[1], Kate Seegmiller[1], Christopher McMahan[2], Rajandeep S. Sekhon[3] and Daniel J. Robertson[1*]

Abstract

Background: Stalk lodging (breaking of agricultural plant stalks prior to harvest) results in millions of dollars in lost revenue each year. Despite a growing body of literature on the topic of stalk lodging, the structural efficiency of maize stalks has not been investigated previously. In this study, we investigate the morphology of mature maize stalks to determine if rind tissues, which are the major load bearing component of corn stalks, are efficiently organized to withstand wind induced bending stresses that cause stalk lodging.

Results: 945 fully mature, dried commercial hybrid maize stem specimens (48 hybrids, ~ 2 replicates, ~ 10 samples per plot) were subjected to: (1) three-point-bending tests to measure their bending strength and (2) rind penetration tests to measure the cross-sectional morphology at each internode. The data were analyzed through an engineering optimization algorithm to determine the structural efficiency of the specimens.

Conclusions: Hybrids with higher average bending strengths were found to allocate rind tissue more efficiently than weaker hybrids. However, even strong hybrids were structurally suboptimal. There remains significant room for improving the structural efficiency of maize stalks. Results also indicated that stalks are morphologically organized to resist wind loading that occurs primarily above the ear. Results are applicable to selective breeding and crop management studies seeking to reduce stalk lodging rates.

Keywords: Computational, Plant, Biomechanics, Modeling, Stalk, Stem, Lodging, Bending, Strength stress, Morphology, Maize, Optimization

Background

Stalk lodging (permanent displacement of plants from their vertical orientation) severely reduces agronomic yields of several vital crop species including maize. Yield losses due to stalk lodging are estimated to range from 5 to 20% annually [6, 16]. Stalk lodging (as opposed to root lodging) occurs when the structural stability of the plant is lost due to structural or material failure of the plant stem [3, 28]. Root lodging occurs when the stalk or stem of the plant remains intact and failure occurs at the root soil interface (i.e., the plant is uprooted). This manuscript is focused on the problem of stalk lodging. Several internal and external factors contribute to a plant's propensity to stalk lodge. External factors include wind speed [38], pest damage [11], disease [10, 22], and canopy airflow [2]. Internal factors include the plant's morphology and material properties [13, 27, 33]. Despite a growing body of literature surrounding the topic of maize stalk lodging, a detailed morphological investigation of the taper of maize stalks has not been reported. The purpose of this paper is to quantify changes in diameter and rind

*Correspondence: danieljr@uidaho.edu
[1] Department of Mechanical Engineering, University of Idaho, 875 Perimeter Dr. MS0902, Moscow, ID 83844, USA
Full list of author information is available at the end of the article

Stubbs *et al. Plant Methods*   (2020) 16:67

Page 2 of 15

thickness of maize stalks as a function of plant height (i.e., taper) and to determine the structural efficiency of the taper of maize stalks. This study investigates stalk taper from a purely structural standpoint to determine the structural efficiency of maize stalks in the absence of external abiotic (i.e., air currents) and biotic (i.e., agronomic management) factors.

To determine the structural efficiency of maize stalks one must both quantify the stalk taper and define probable wind loading scenarios. An efficiently tapered stalk is defined as one in which uniform mechanical stresses are produced when the plant is subjected to probable wind loading scenarios. In other words, the shape of the stalk is optimal, meaning that loads are supported with as little tissue as possible. An inefficient taper is one in which non-uniform mechanical stresses are produced. Inefficient stalks utilize more structural tissue than is necessary in some areas and less structural tissue than is necessary in other areas to withstand the loads to which they are subjected. In other words, for inefficient stalks the amount of structural tissue could be reduced without affecting the load bearing capacity of the stalk. The structural efficiency of maize stalks is of interest because efficient stalks would theoretically have more available biomass and bioenergy to devote to grain filling as compared to inefficient stalks (i.e., efficient stalks would have a higher harvest index).

As mentioned previously, both the taper and probable wind loading scenarios must be defined to determine the structural efficiency of maize stalks. The wind load exerted on a plant stalk, known as the drag force (D_f), can be approximated as [25]:

$$D_f = 0.5\rho u^2 A_p C_D \tag{1}$$

where ρ is the density of air, u is the local wind speed, A_p is the projected area of the structure, and C_D is the drag coefficient. While this equation appears fairly simple at first glance, it is complicated by the fact that the variables on the right-hand side of the equation are functions that can vary both temporally and spatially. For example, the drag coefficient changes spatially along the length of the stalk and is also a function of the local wind speed. As the local wind speed increases, the angle of the leaf blades and tassel change (known as flagging), which alters the drag coefficient [3, 25].

The strong interrelationships between the factors of Eq. 1 complicate attempts to directly measure wind forces on maize stalks. Direct measurements of wind speeds have successfully been used to estimate drag forces in past studies of trees and cereal crops [25, 26, 36]. However, the large ratio of leaf area to stalk area, close proximity of maize plants to one another in commercial fields, and other confounding factors imply that a direct measurement of the wind speed near a maize stalk is not necessarily a good predictor of the drag force experienced by the stalk. Detailed computational engineering models that capture the interplay between fluid dynamics and structural deformations (i.e., fluid–structure interaction models [41]) could potentially be used to calculate the drag force experienced by maize stalks over time. However, such models are highly complex and computationally expensive, due to difficulties in estimating the constantly changing drag force and orientation of the plant tissues (projected area) with respect to wind vectors that vary in three dimensions. In summary, accurately measuring drag forces in crop canopies is challenging and remains an active area of research. An overview of this topic is given by Finnigan [15].

While direct measurement of exact wind forces on maize stalks is challenging, defining the realm of probable wind loading scenarios is less so. To define the realm of probable wind loading scenarios we assume the wind speed acts in the same direction along the length of the stalk. In other words, the wind does not blow in one direction at the bottom of the stalk and in a different direction at the top of the stalk. Although there are times when hairpin eddies can form as air circulates through the canopy [14], the assumption of uniform wind direction was made for purposes of the optimization algorithm used in this study. This assumption is described in more detail in "Limitations" section. We can also bound the degree of change in the magnitude of the wind force along the length of the plant. For example, previous studies and engineering fluid mechanics theory dictate that the local wind speed in crop canopies increases with height [9, 38, 39]. A simple examination of corn stalks also suggest that the combination of the drag coefficient and projected area increases with plant height (i.e., the leaves near the bottom of mature maize plant are often dead and fall off whereas the top leaves remain structurally robust). Thus both the local wind speed and the combined effect of the drag coefficient and projected area can be assumed to increase with plant height. Combining these insights with Eq. 1, we can determine that the wind force (i.e., drag force) increases with plant height (at a time prior to stem deflection). The stalk lodging resistance of a plant can be defined as the plants ability to withstand these externally applied loadings. We can therefore gain insights into a plant's stalk lodging resistance by looking at a bounded range of potential wind-loading scenarios. At the upper bound of probable wind loading we assume all of the wind force acts at the top of the plant as a point load [17]. At the lower bound of probable wind loading we assume a uniform load is applied to stalk along its entire length (i.e., the drag force at the top of the plant is the same as the drag force in every other cross-section of the plant including the bottom of the plant). These bounds allow for all probable wind-loading scenarios and exclude improbable scenarios. Figure 1

Stubbs *et al. Plant Methods*   (2020) 16:67

Page 3 of 15

visually represents each of these assumptions. For example, probable wind loading profiles such as a quadratic increase in wind loading from the bottom to the top of the plant, would fall within the white region of Fig. 1-top. Conversely, improbable wind loading profiles, such as the drag force being higher at the base of the plant than at the top of the plant, would fall outside of the white region in Fig. 1-top.

The structural efficiency of maize stalks can be determined by using Engineering equations that relate stem morphology and mechanical stress to probable wind loading scenarios presented in Fig. 1. In particular, the maximum stress in any cross-section (σ) (typically presented in units of Pascal) due to wind-induced bending is calculated as [4]:

$$\sigma = \frac{\int_0^L D_f \, dx}{S_x} \tag{2}$$

where D_f is the drag force (see Eq. 1) and S_x is the section modulus (typically presented in units mm^3) at a distance x along the stalk, and L is the length of the stalk. Section modulus is an engineering term that quantifies the morphology of the cross-section [4]. Perhaps somewhat surprisingly, Eq. 2 does not include an elastic modulus term or any other material or tissue property terms. This
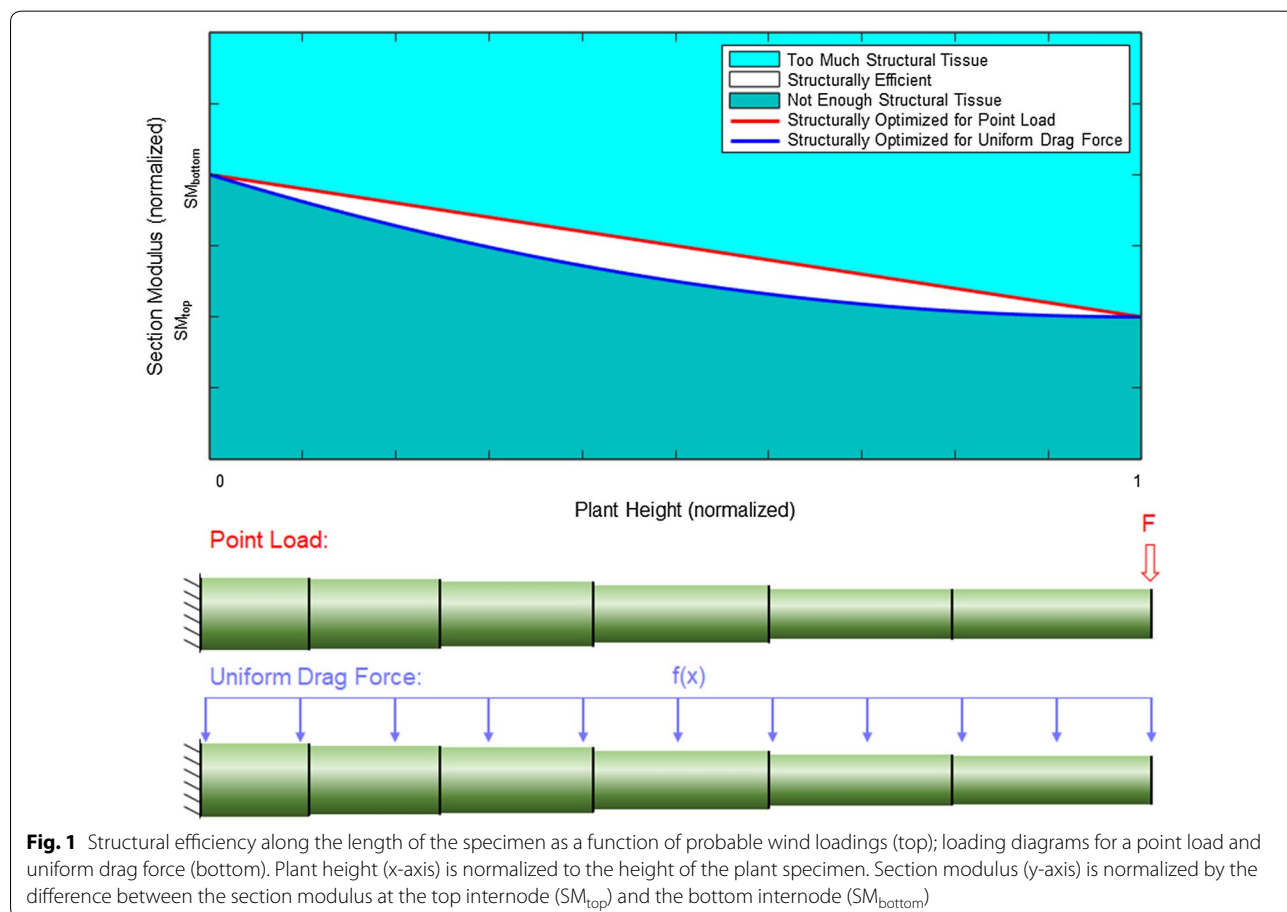
is because for a structure with a single homogeneous linear elastic orthotropic material, the relationship between external applied loads and stress is independent of material properties.

Maize stalks possess elliptical cross-sections, therefore, the section modulus of each cross-sections is a function of the ellipse's major diameter (D), minor diameter (d), and the thickness of the rind (t) in the form [40]:

$$S_x = \frac{\pi}{32d}\Big(Dd^3 - (D - t)(d - t)^3\Big). \tag{3}$$

By combining Eqs. 2 and 3, we can calculate the drag force and section modulus combination that results in a uniform stress along the length of the plant.

Figure 1-top displays a visual representation of the range of possible tapers for maize stalks that could produce uniform stresses during probable wind loading scenarios. In other words, it displays the combination of external loadings and section moduli that Eq. 2 dictates would result in uniform stress along the length of the stem. The range of probable wind loadings is defined with an upper bound (red curve) of a point load applied to the top of the plant, and a lower bound (blue curve)

Fig. 1 Structural efficiency along the length of the specimen as a function of probable wind loadings (top); loading diagrams for a point load and uniform drag force (bottom). Plant height (x-axis) is normalized to the height of the plant specimen. Section modulus (y-axis) is normalized by the difference between the section modulus at the top internode (SM_{top}) and the bottom internode (SM_{bottom})

Stubbs *et al. Plant Methods*   (2020) 16:67

Page 4 of 15

of a uniform drag force applied to the entire length of the specimen. The graph depicts the most efficient plant tapers (white area) from the ground ($x = 0$) to the top of the plant specimen ($x = 1$), and from the section modulus at the uppermost internode of the plant specimen ($y = SM_{top}$) to the section modulus at the bottommost internode of the plant ($y = SM_{bottom}$). If the section modulus of an internode falls above the red curve, then that internode will experience a lower maximum stress than the rest of the plant, as it has more structural tissues (i.e., mass) than is necessary. If the section modulus of an internode falls below the blue curve, then that internode will experience a higher maximum stress than the rest of the internodes of the plant, as it has less structural tissue than is efficient. If the section modulus of an internode falls between the red and blue curves (white area), then that internode will experience a similar level of mechanical stress as compared to the rest of the plant, and therefore has an efficient allocation of structural tissues.

To determine the structural efficiency of maize plants, a select group of maize stalks were analyzed. Their major and minor diameters and rind thicknesses were measured at each internode and compared to Fig. 1. In addition, a custom optimization algorithm was employed to determine the exact drag force profile for each plant that would produce the most uniform mechanical stress possible for the given stalk structure. The details and results of these experiments are presented in the following sections.

Box 1: Glossary of terms

Term	Definition
A_p	Projected area of the structure
C_D	Drag coefficient
D	Major diameter of the cross-section
d	Minor diameter of the cross-section
D_f	Drag force
F_0	Positive resolved force applied to the top of the specimen
f(x)	Loading profile along the length of the specimen
M_0	Positive resolved moment applied to the top of the specimen
S_x	Section modulus at the location x along the length of the specimen
s	Bending stress vector for optimization algorithm
σ	Bending stress
ρ	Density of air
t	Rind thickness
u	Local wind speed
v	Residual vector for optimization algorithm
X	Input loading vector for optimization algorithm
x	Length along the length of the specimen
Y	Total residual scalar for optimization algorithm

Methods

All maize specimens in this study were subjected to the following battery of tests. First, major and minor diameters of each internode were measured with calipers and internode lengths were measured with a ruler. Second, bending strength was measured in three-point bending. Third, rind thickness was measured through rind penetration tests [29]. Each stalk was then analyzed, and an optimization algorithm was employed to determine the theoretical drag force profile that would produce the most uniform stresses along the entire length of the stalk. Finally, statistical analyses were performed to investigate the relationship between each specimen's strength and its structural efficiency.

Plant materials

Forty-eight maize hybrids, chosen to represent a reasonable portion of maize genetic diversity, were evaluated for variation in stem morphology and structural tissue distribution. The hybrids were planted at Clemson University Simpson Research and Education Center, Pendleton, SC in well drained Cecil sandy loam soil. The hybrids were grown in a Random Complete Block Design with two replications. In each replication, each hybrid was planted in two-row plots with row length of 4.57 m and row-to-row distance of 0.76 m with a targeted planting density of 70,000 plant ha^{-1}. The experiment was surrounded by non-experimental maize hybrids on all four sides to prevent any edge effects. To supplement nutrients, 56.7 kg ha^{-1} nitrogen, 86.2 kg ha^{-1} of phosphorus and 108.9 kg ha^{-1} potassium was added at the time of soil preparation, and additional 85 kg ha^{-1} nitrogen was applied 30 days after emergence. Standard agronomic practices were followed for crop management.

Stalks used for this study were harvested when all the hybrids were either at or past physiological maturity (i.e., 40 days after anthesis), determined based on our previous studies on senescence and patterns of sugar accumulation in maize [30]. Ten competitive plants (i.e., plants free of disease and of structural damage) from each replication were harvested by cutting at just above ground level, stripped of all the leaves and ears, and transferred to a forced air dryer for drying at 65 °C. Some plots lacked 10 competitive plants (i.e., lacked 10 plants that were structurally robust enough to be tested) and, therefore, the total number of plants evaluated for each hybrid varied slightly. In total, 945 fully mature, dried commercial hybrid maize stalks were used in this study (48 hybrids, ~2 replicates, ~10 samples per hybrid).

Stubbs *et al. Plant Methods* (2020) 16:67

Page 5 of 15

Three-point-bending tests

Specimens were tested in three-point-bending using an Instron Universal Testing System (Instron Model # 5944, Norwood, MA). Specimens were supported at their bottom and top node, and loaded at their middle node. Care was taken to ensure that the specimens were both loaded and supported at nodes, and that the span lengths were maximized. This was done to obtain the most natural possible failure modes [28, 33]. Specimens were loaded at a rate of 2 mm s^{-1} until structural failure. Additional details on the three-point-bending test protocol were documented in a previous study [27]. Short span 3-pt bend tests (i.e., testing of a single internode with supports placed at adjacent nodes) were not employed in this study as they have been shown to produce unnatural failure patterns and result in inaccurate bending strength measurements [28].

Morphology measurements

Internode lengths of each specimen were measured with a ruler. Other morphology measurements were taken at the midspan of each internode of every specimen. In particular, caliper measurements were used to obtain the minor and major diameters of each internode. Rind penetration tests were used to obtain the rind thickness of each internode. Rind penetration tests were performed using an Instron universal testing machine at the midspan of each internode of every specimen. A probe was briefly forced through the specimen at a rate of 25 mm s^{-1}, and the resulting force–displacement curve was analyzed using a custom MATLAB algorithm to calculate the rind thickness (t) of the stalk cross-section. Additional details on the rind penetration test protocol are documented in Seegmiller et al. [29].

Optimization of loading condition

An optimization algorithm was employed to determine the drag force profile (f(x)) for each stem specimen that would produce the most uniform stress along the length of the stalk. As the specimens examined only spanned the bottom half of the stalk (from the ground to the ear), the loading above the ear was resolved into a single positive force (F_0) and positive moment (M_0) applied to the top of the specimen as described by Beer et al. [4] and shown in Fig. 2. For the hybrids investigated, the ear was an average of 46.1% ($\pm$7.72% standard deviation; 95% confidence interval around the mean [45.46%, 46.76%]) of the way up the stalk.

Based on this setup, we can now calculate the single positive resolved force applied to the top of the specimen (F_0) and the loading profile (f(x)) for each specimen that results in the most uniform stress state in each particular specimen. This was accomplished through the use of an optimization algorithm. In particular, a custom code was developed in Matlab to perform an *fmincon* optimization for each stem specimen [7, 20, 32]. The optimization algorithm *fmincon* is a function that finds a minimum of a constrained nonlinear multivariate function. This optimization function was used to minimize the variation in mechanical stress across the length of the specimen by changing the values of the input parameters F_0 and f(x) (see Fig. 3). In other words, the algorithm found the loading condition that produced the most uniform stress along the entire length of the stem. To accomplish this, each specimen was computationally partitioned into 100 cross-sections and the optimization routine would then: (1) take in user-supplied initial estimations of F_0 at the top of the specimen and f(x) at the other 99 cross-sections (100×1 vector X), (2) calculate bending stress at every cross section using Eq. 2 (100×1 vector s), (3) calculate the variance between the bending stress at each cross-section and the uniform stress state (i.e., the distance between the "Uniform Stress State" and "Stress State Resulting from *fmincon* Optimization Procedure" curves in Fig. 3), (100×1 vector v), (4) sum all the elements of vector v (i.e., the total area between the "Uniform Stress State" and "Stress State Resulting from *fmincon* Optimization Procedure" curves in Fig. 3) (scalar value Y), (5) iterate on X until the variance Y was
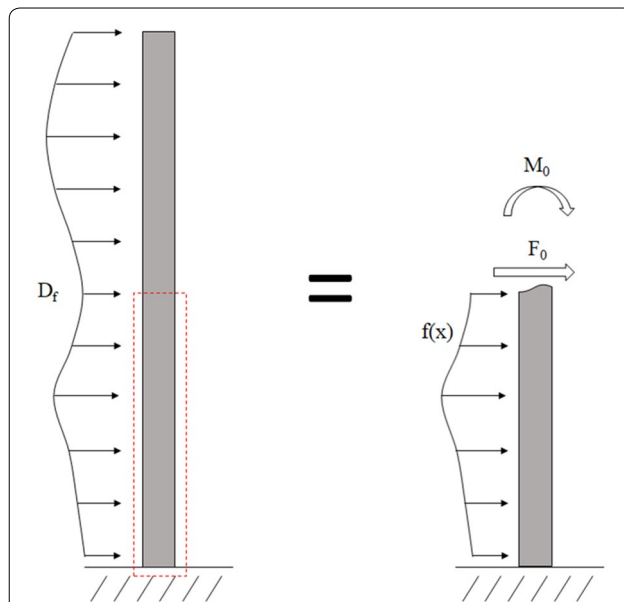

Fig. 2 A loading diagram of the wind on the plant stalk with an unknown load distribution along the length of the stalk (left); the wind loading above the ear can be resolved as an unknown positive force (F_0) and positive moment (M_0) applied to the top cross section (right) [4]
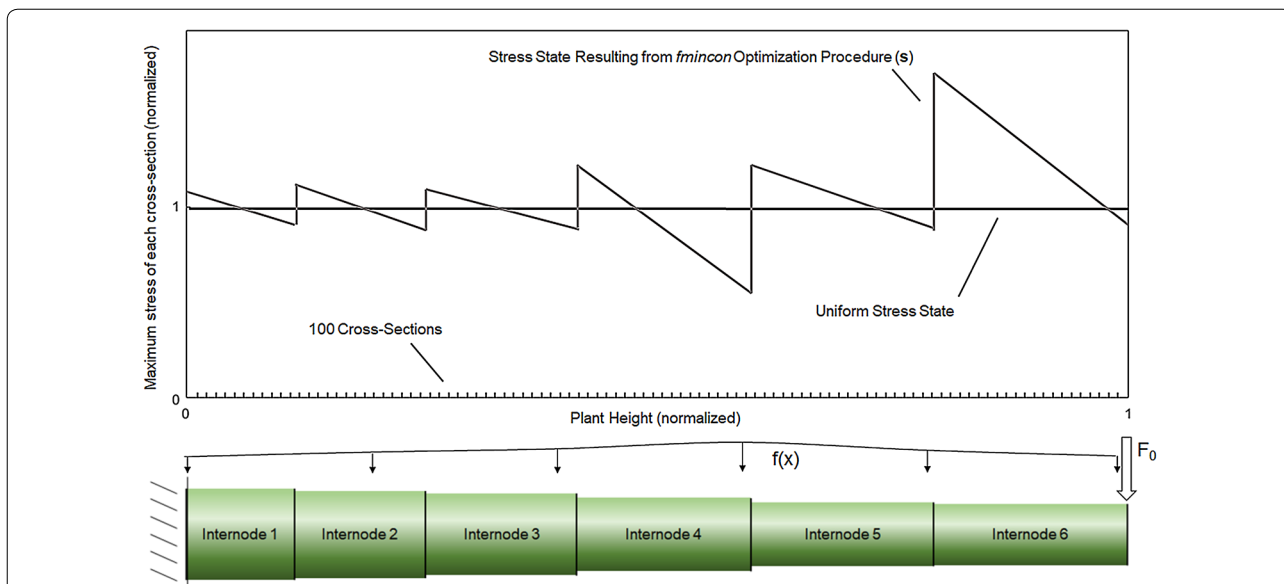
Fig. 3 A typical specimen output, showing the stress state resulting from the fmincon optimization procedure, which attempts to create the most uniform possible stress state along the length of the specimen by altering values for F_0 and f(x) (top); the analytical maize stalk model partitioned into 100 cross-sections along its length (bottom). Plant height (x-axis) is normalized to the height of the plant specimen. Maximum stress of each cross-section (y-axis) normalized to a target stress of 1.00
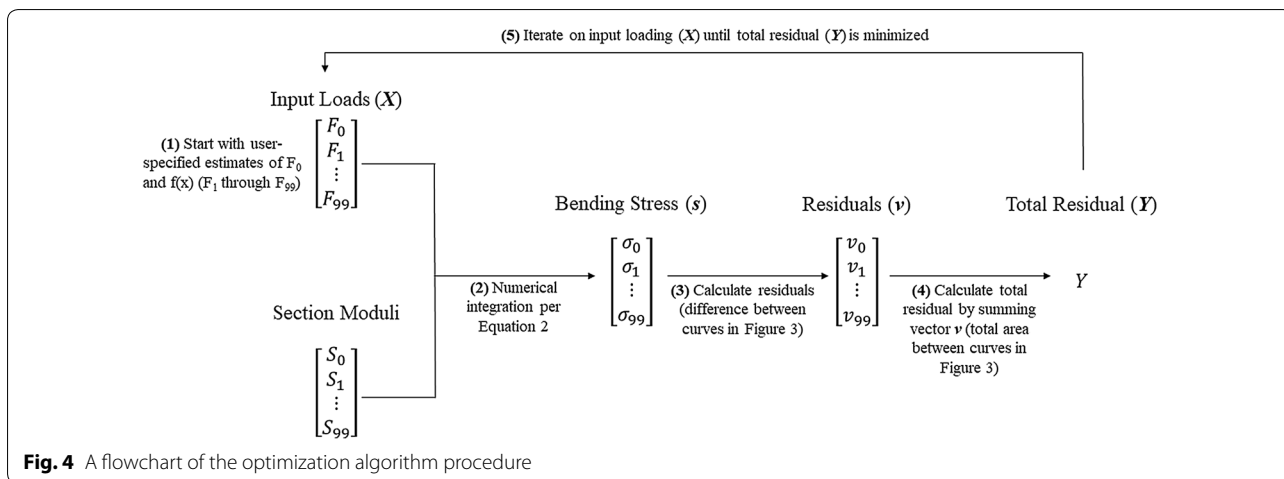

Fig. 4 A flowchart of the optimization algorithm procedure

minimized. The code would then give the drag force profile X that produced the most uniform stress state along the specimen (s), and the total variance in the bending stress (Y), which is a quantitative assessment of how efficiently the specimen's structural tissues (i.e., rind) were allocated. Figure 4 presents a visual depiction of this optimization procedure. The optimization routine was conducted with several different initial starting points for each specimen (i.e., initial values for F_0 and f(x)) to ensure the global optimal solution was found as opposed to a local minimum. Tolerances and stopping criteria were set to 1E−6 (first order optimality tolerance), 1E−6

(function tolerance), and 1E−10 (step size tolerance) [24].

Results

Both the three-point-bending tests and rind penetration tests yielded the expected results, based on previous studies [27, 28, 33]. The three-point-bending force–deflection responses were linear in nature until failure and demonstrated failure patterns that occur in naturally lodged maize plants [28, 33]. The rind penetration tests gave results characteristic of the protocol. The bending strength of each specimen, as well as the section

Stubbs *et al. Plant Methods*   (2020) 16:67

Page 7 of 15

modulus, length, major diameter, minor diameter, and rind thickness of each specimen internode is presented in Fig. 5.

Structural efficiency

Section modulus values for each stalk were analyzed to determine structural efficiency (i.e., how structurally efficient the taper of each stalk was). The median taper of the population was calculated by determining the median section moduli at each specimen height, among all specimens. It was found that the median taper of all stalks demonstrated an efficient allocation of structural tissues for probable wind loadings (see Fig. 6). However, many internodes fell well outside the range of structural efficiency (i.e., outside of the white area in Fig. 6). In particular, 35% of the measured internodes in the study fell within the most efficient range, 38% of measured internodes fell below the blue curve (too little structural tissue), and 27% of the measured internodes fell above the red curve (too much structural tissue).

Optimal drag force profile for each stalk

The optimization procedure was performed on all 945 stalks. The *fmincon* procedure successfully determined the drag force profile (X) that produced the most uniform stress state for each specimen. Figure 7 depicts histograms of the resulting stress states of the specimens. In particular, the overall average stress along the length of each specimen (n = 945) and the stress at every cross-section of each specimen (n = 94,500) is presented in Fig. 7. To enable all specimens to be plotted on the same graph the stress of each specimen/cross-section was normalized to a target stress of 1.00. In other words, a stress state different than a stress of 1.00 represents a suboptimal allocation of structural tissues.

Are stronger stalks more efficient?

To test the hypothesis that stronger plants allocate structural tissues more efficiently (i.e., they produce uniform stresses under probable wind loading scenarios), a series of statistical analyses were performed on the data. Figures 8 and 9 provide a depiction of the variation (via boxplots) in bending strength and structural efficiency measurements stratified by hybrid type. Figures 10 and 11 provide the same but further stratified by hybrid type and replication. As discussed previously, the level of structural efficiency can be determined by calculating the area between the curves shown in Fig. 3 (Y). For example, a Y value of zero represents a perfectly efficient structure, and the larger the Y value, the less efficiently the stalk tissues are organized. These figures indicate substantial variation in bending strength and structural efficiency across

hybrids. Moreover, these measures vary within hybrid type; i.e., across replication. To formally examine this, we posit a model of the following form:
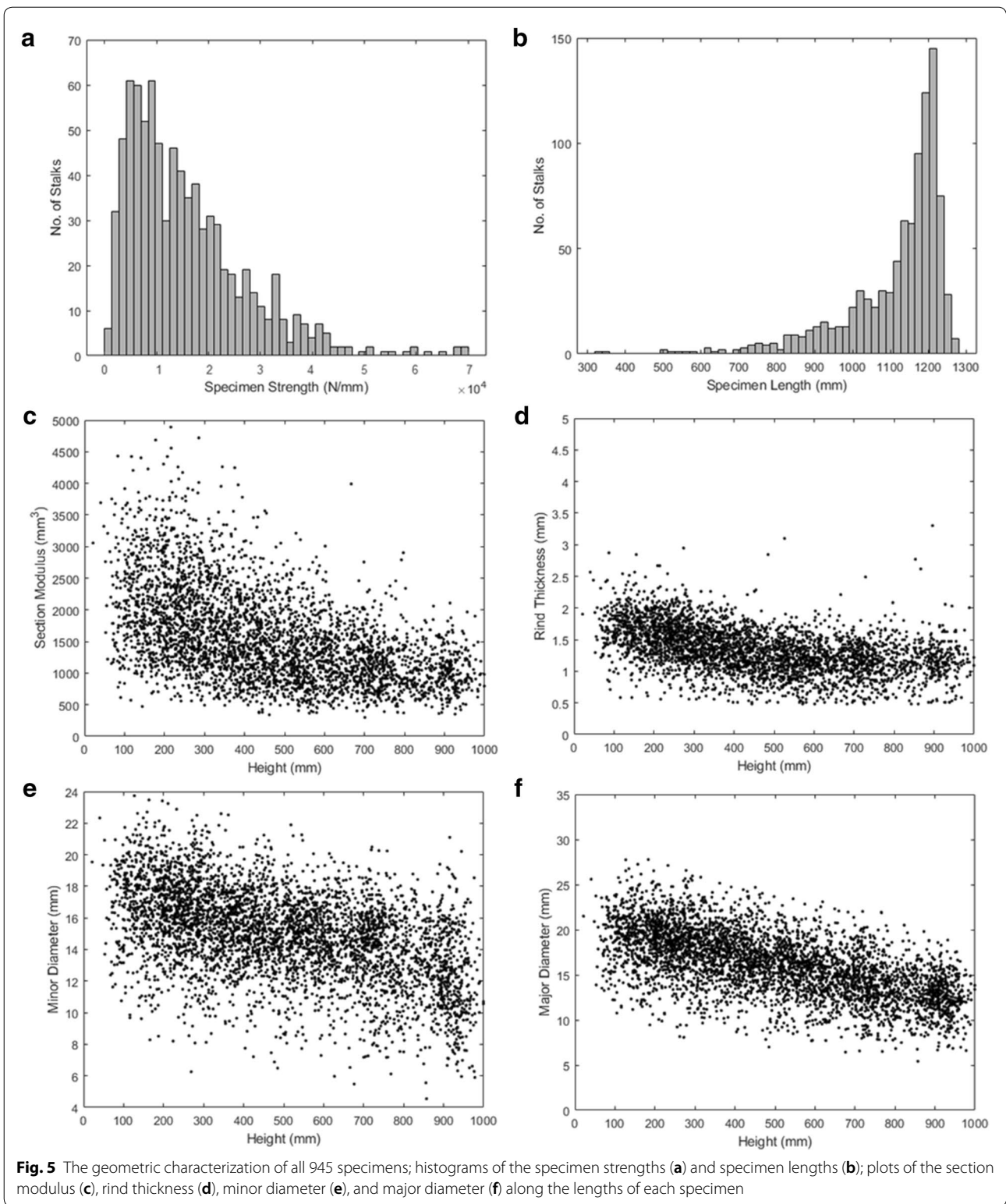
$$Y_i = \beta_0 + \sum h_{ij}\beta_j + r_i\alpha_0 + \sum r_i h_{ij}\alpha_k + \varepsilon_i, \qquad (4)$$

where Y_i is the response variable of interest (e.g., log transformed bending strength ($\log(\sigma)$) and log transformed efficiency ($\log(Y)$)) as measured on the ith observation, β_0 is an intercept parameter, h_{ij} is a dummy variable that encodes the hybrid type (i.e., if the ith observation was taken on a plant belonging to the jth hybrid then $h_{ij} = 1$ and $h_{ij'} = 0$ for all $j' \neq j$), β_j is the effect associated with the jth hybrid, r_i is a dummy variable that encodes replication (i.e., if the ith observation was taken on a plant grown in replication 1 then $r_i = 1$ and $r_i = 0$ otherwise), α_0 is the replicate effect, and ε_i is the error term. To avoid identifiability issues, the dummy variables were constructed with respect to a chosen hybrid baseline. Tables 1 and 2 summarize the findings of this analysis. In particular, these tables display the ANOVA results as obtained from the *anova* function in R; which present the usual sequential sums of squares, where p-values are for the tests that compare the models against one another in the order specified. From these results we find that hybrid type (p-value ≤ 2e−16), replicate (p-value = 0.000285), and their interaction (p-value ≤ 2e−16) are highly significant for log-strength. Similarly, for log-efficiency we find that both hybrid type (p-value = < 2e−16) and the interaction term between hybrid type and replicate (p-value = 1.46e−05) are highly significant, while replicate (p-value = 0.0882) is not. These findings indicate that both genetics (i.e., hybrid type) and environment (i.e., plot location) are associated with bending strength and structural efficiency. It is worthwhile to point out that standard model diagnostics (e.g., residual plots, QQ-plots, etc.) were conducted to assess the validity of each of these models, as well as those discussed below.

Delving deeper, we consider the regression analysis of log-efficiency (denoted Y_i) under the following multiple linear regression model:
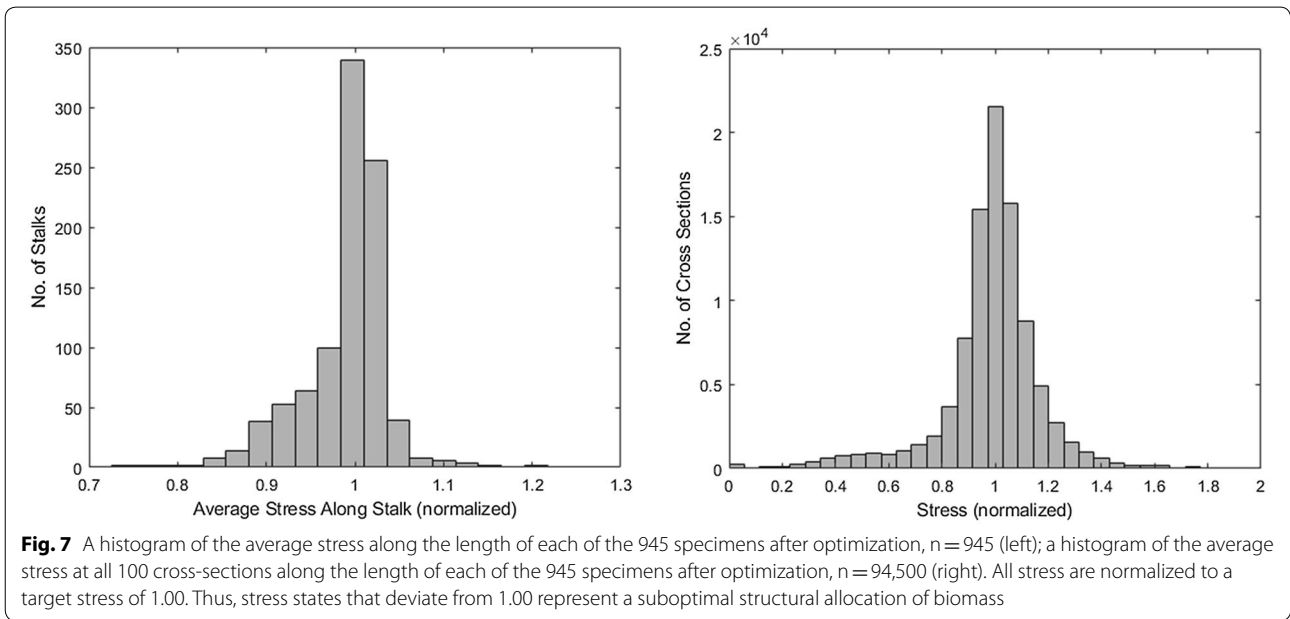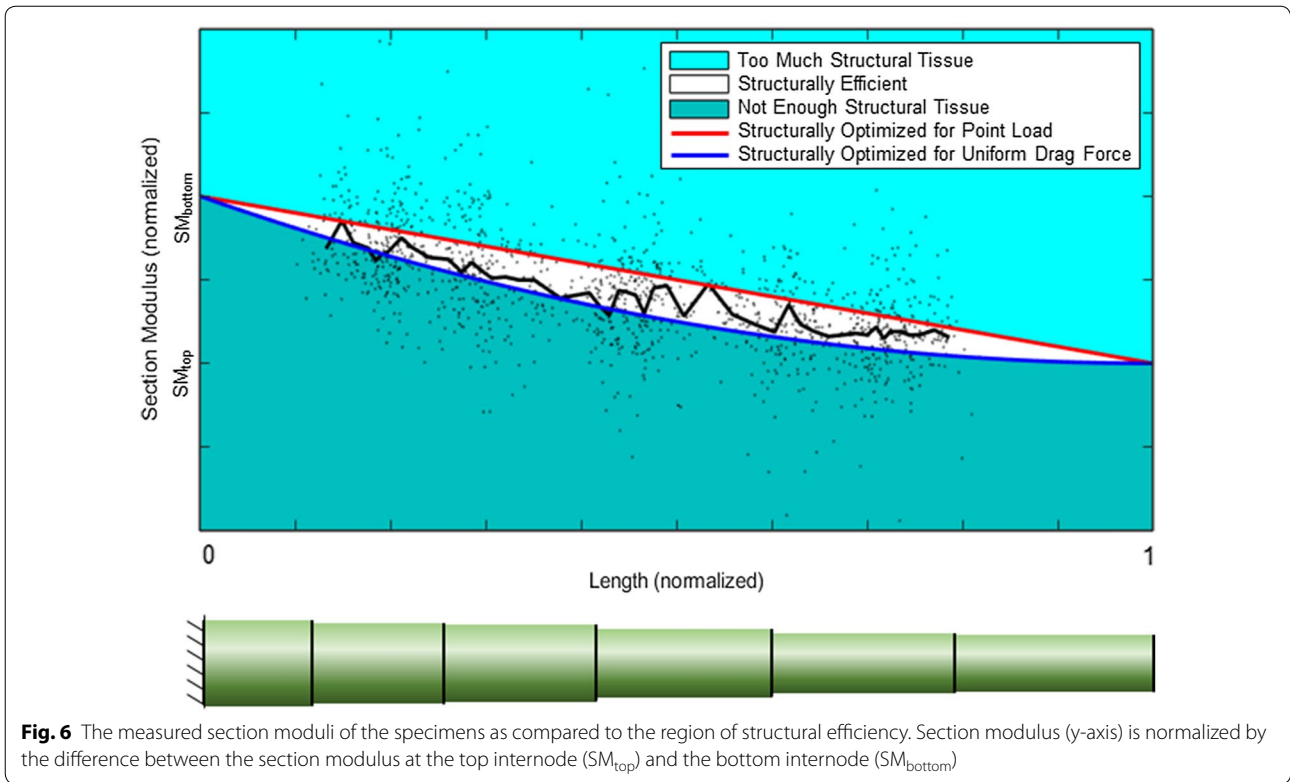
$$Y_i = \beta_0 + S_i\delta_1 + S_i^2\delta_2 + \sum h_{ij}\beta_j + r_i\alpha_0 + \sum r_i h_{ij}\alpha_k + \varepsilon_i, \qquad (5)$$

where $S_i(S_i^2)$ denotes the strength (squared) of the ith observation and $\delta_1(\delta_2)$ denotes the corresponding effect size. Note, strength was entered into the model in a quadratic form due to the findings of model diagnostics. Table 3 presents a summary of this analysis. This table displays the ANOVA results as obtained from the *anova* function in R. From these results we see that strength is significantly related to efficiency, even when controlling
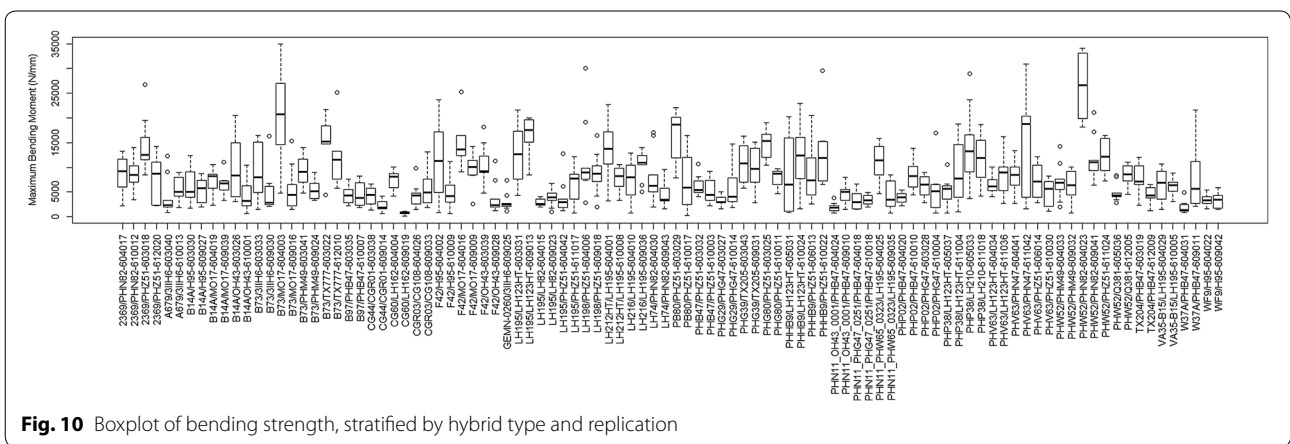
Stubbs *et al. Plant Methods*   (2020) 16:67

Page 8 of 15

Fig. 5 The geometric characterization of all 945 specimens; histograms of the specimen strengths (**a**) and specimen lengths (**b**); plots of the section modulus (**c**), rind thickness (**d**), minor diameter (**e**), and major diameter (**f**) along the lengths of each specimen

for hybrid type, replication, and their interaction. When conducting the individual tests of significance (results not shown) about δ_1 and δ_2 we have the p-values $< 2e-16$ and $1.81e-07$, respectively; i.e., strength seems to be

significantly (quadratically) related to efficiency, while controlling for hybrid type, replication, and their interaction. Further, we see that hybrid type, replicate, and their interaction continue to be highly significant for

Stubbs *et al. Plant Methods*   (2020) 16:67

Page 9 of 15

Fig. 6 The measured section moduli of the specimens as compared to the region of structural efficiency. Section modulus (y-axis) is normalized by the difference between the section modulus at the top internode (SM_{top}) and the bottom internode (SM_{bottom})

Fig. 7 A histogram of the average stress along the length of each of the 945 specimens after optimization, n = 945 (left); a histogram of the average stress at all 100 cross-sections along the length of each of the 945 specimens after optimization, n = 94,500 (right). All stress are normalized to a target stress of 1.00. Thus, stress states that deviate from 1.00 represent a suboptimal structural allocation of biomass

log-efficiency. This tends to suggest that other genetic components and environmental conditions might be at play with respect to fully explaining the structural efficiency of maize stalks. The R^2 (adjusted R^2) for this model was 0.5139 (0.4493).

For completeness, we also conducted the regression analysis of the section modulus of the 2nd and 3rd internode down from the ear. This analysis was done using a model of the form:

Fig. 8 Boxplot of bending strength, stratified by hybrid type

Fig. 9 Boxplot of structural efficiency, stratified by hybrid type

Fig. 10 Boxplot of bending strength, stratified by hybrid type and replication
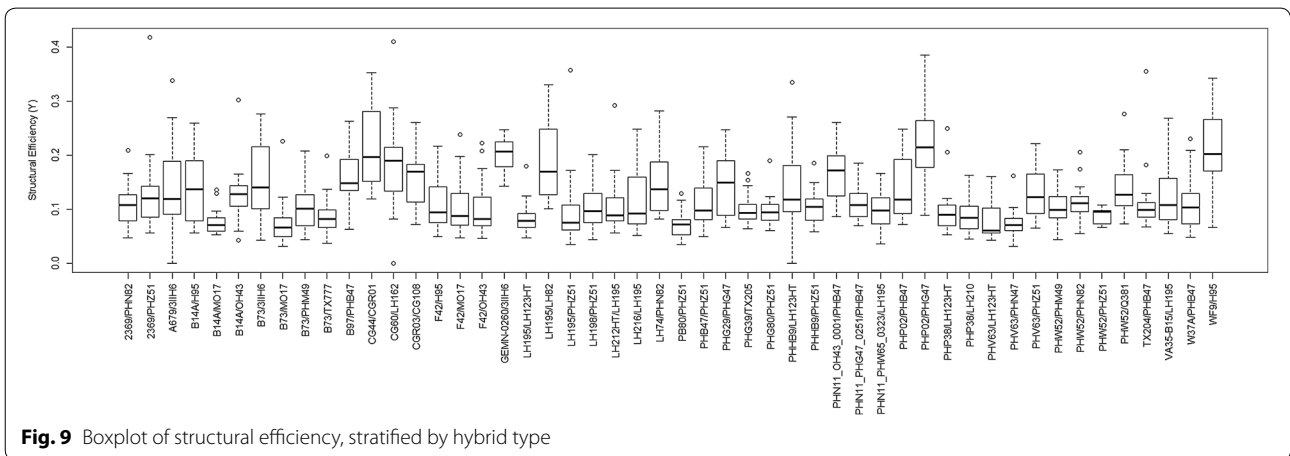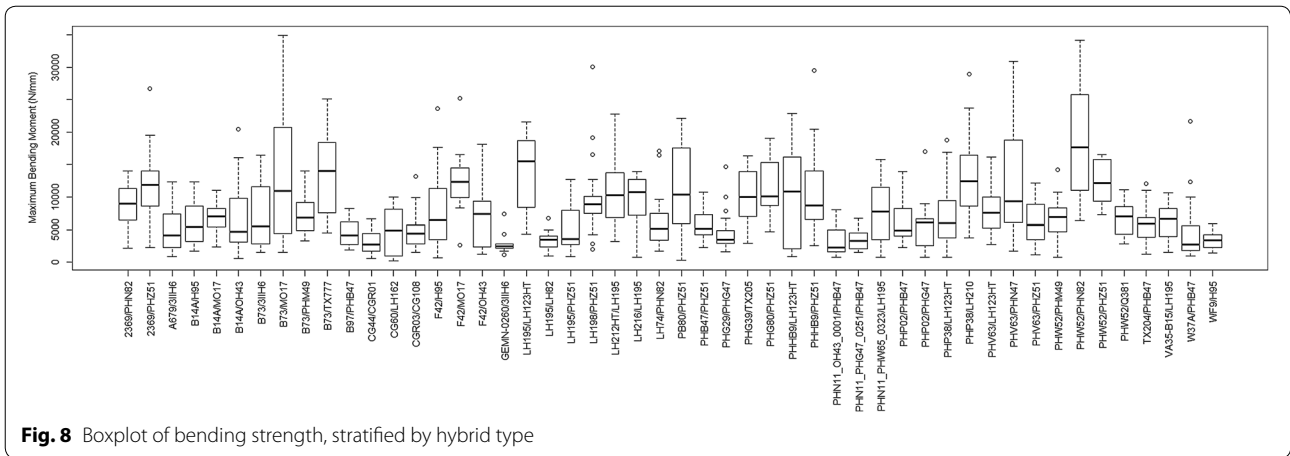
$$Y_i = \beta_0 + \sum h_{ij}\beta_j + r_i\alpha_0 + \sum r_i h_{ij}\alpha_k + \varepsilon_i, \qquad (6)$$

where Y_i again represent the response of interest (i.e., log transformed section modulus of the 2nd and 3rd

internode) as measured on the ith observation, with all other variables being defined as above. Tables 4 and 5 report the results of the analysis of the section modulus of the 2nd and 3rd internodes, respectively. From these
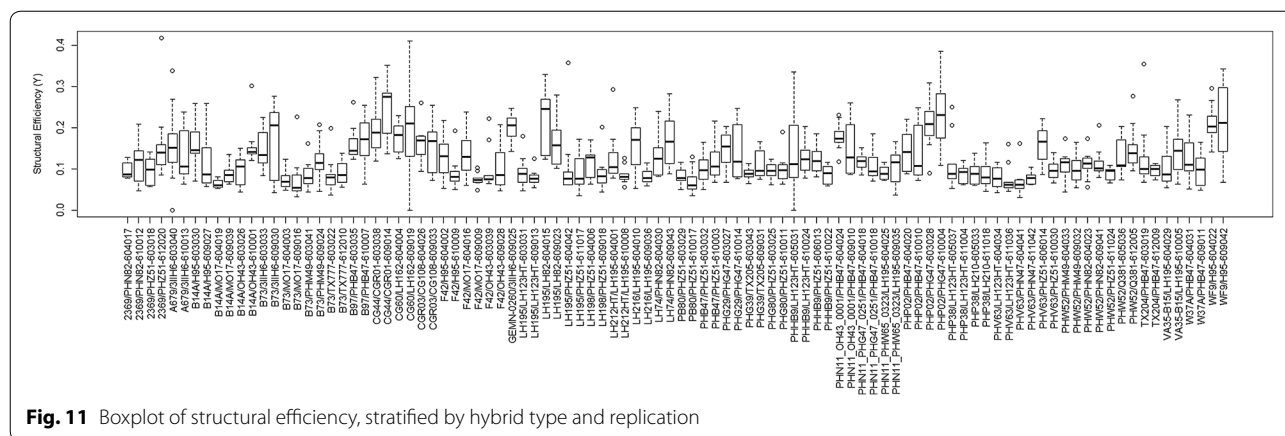
Stubbs *et al. Plant Methods*   (2020) 16:67

Page 11 of 15

Fig. 11 Boxplot of structural efficiency, stratified by hybrid type and replication

Table 1 Results of analysis for log(strength)

Variable	Df	Sum sq.	Mean sq.	F-value	p-value
H	49	169.46	3.458	9.203	<2e−16
R	1	4.99	4.994	13.290	0.000285
H*R	47	88.23	1.877	4.995	<2e−16
Residual	750	281.84	0.376		

Table 2 Results of analysis for log(Y)

Variable	Df	Sum sq.	Mean sq.	F-value	p-value
H	49	75.96	1.5502	10.823	<2e−16
R	1	0.42	0.4173	2.913	0.0882
H*R	47	14.62	0.3112	2.172	1.46e−05
Residual	844	120.89	0.1432		

Table 3 Results of analysis for log(Y) regression

Variable	Df	Sum sq.	Mean sq.	F-value	p-value
S	1	30.06	30.058	247.798	<2e−16
S^2	1	8.03	8.034	66.234	1.68e−15
H	49	41.08	0.838	6.912	<2e−16
R	1	1.04	1.041	8.582	0.0035
H*R	47	15.31	0.326	2.686	2.57e−08
Residual	745	90.37	0.121		

results, we find that hybrid type and the interaction term between hybrid type and replicate are highly significant, while replicate is not for log-section modulus of both internodes.

Table 4 Results of analysis for log(section modulus) for internode 2

Variable	Df	Sum sq.	Mean sq.	F-value	p-value
H	49	66.30	1.3531	13.470	<2e−16
R	1	0.05	0.0480	0.477	0.49
H*R	47	18.87	0.4016	3.998	<2e−16
Residual	841	84.48	0.1005		

Table 5 Results of analysis for log (section modulus) for internode 3

Variable	Df	Sum sq.	Mean sq.	F-value	p-value
H	49	73.34	1.4968	14.678	<2e−16
R	1	0.22	0.2209	2.166	0.141
H*R	47	23.05	0.4904	4.809	<2e−16
Residual	842	85.86	0.1020		

Discussion

Improving structural efficiency in maize plants could simultaneously enhance yield and stalk lodging resistance. However, there has not been any previous investigations of structural efficiency in maize stalks. Consequently, plant scientists have not directly breed or managed for plants that are structurally optimized. Results from this study suggest that the majority of modern maize hybrids may possess suboptimal stalk structures (see Fig. 6). In other words, most maize plants utilize bioenergy and structural biomass inefficiently. This reduces the amount of potential biomass and bioenergy available for grain filling (i.e., lowers harvest index) and simultaneously makes stalks more susceptible to stalk lodging. Of the 945,000 cross-sections analyzed in this study 65% were structurally suboptimal with 38%

having too much structural tissue and 27% having too little structural tissue.

Analysis of the drag force profiles for each specimen that would produce the most uniform stress in the specimen revealed that the resolved force F_0 was far larger than the drag force profile below the ear (see Fig. 12). These data imply that stalks allocate structural tissues for wind loading that primarily occurs above the ear (e.g., the drag force increases exponentially with height). This does not imply that there is no wind below the ear, but that the drag force (determined by the local wind speed, projected stalk and leaf area, and drag coefficient) is much less below the ear as compared to the drag force above the ear. Note this does not imply the bending stresses are lower at the base of the stalk. Bending stresses are determined by forces (i.e., f(x) and F_0) and moment arms (i.e., distance at which the force is applied). Thus, bending stresses are always higher at the base of the stalk even if the drag force profile is lower at the base of the stalk.

Three-point bending tests are the most commonly employed test to quantify bending strength in plant stalks [28, 33, 34]. However, results from this study highlight several shortcomings of the three-point-bending test approach. In particular, most plant stalks are tapered and researchers typically opt to place the loading anvil

from a three-point-bending test at the same anatomical location for each stem specimen in a given study (e.g., the third internode). Thus, the failure location is artificially imposed by the researcher since failure always occurs near the loading anvil, whereas in nature, the failure location is determined by local material weakness and imperfections (i.e., suboptimal allocation of structural tissues). By artificially imposing the failure location the researcher is inducing failure in a cross-section that may have more structural tissue than is optimal in some specimens and less structural tissue than is optimal in other specimens. This confounds comparisons of bending strength among different specimens in a given study, as the measured bending strength could vary substantially for any given specimen depending on the structural optimality of the failed cross-section. A better approach is to apply bending loads that replicate natural loading patterns. Such loading conditions produce natural failure types and failure patterns in plant specimens (i.e., failure occurs at the cross-section with the least optimal allocation of structural tissue). Several devices have been recently developed which accomplish this task [5, 8, 12, 18, 19, 21, 30]. In particular, they utilize the natural anchoring of the maize roots and apply a point load to a cross-section near the ear (very similar to the loading profile shown in

Fig. 12 The drag force profile for all 945 specimens (f(x) and F_0) (top); a loading diagram of f(x) and F_0 (bottom). The 75th and 25th percentile values are generally line-on-line with the median values along the length of the specimen. Plant height (x-axis) is normalized to the height of the plant specimen. Force (y-axis) is normalized to the maximum calculated force

Stubbs *et al. Plant Methods*   (2020) 16:67
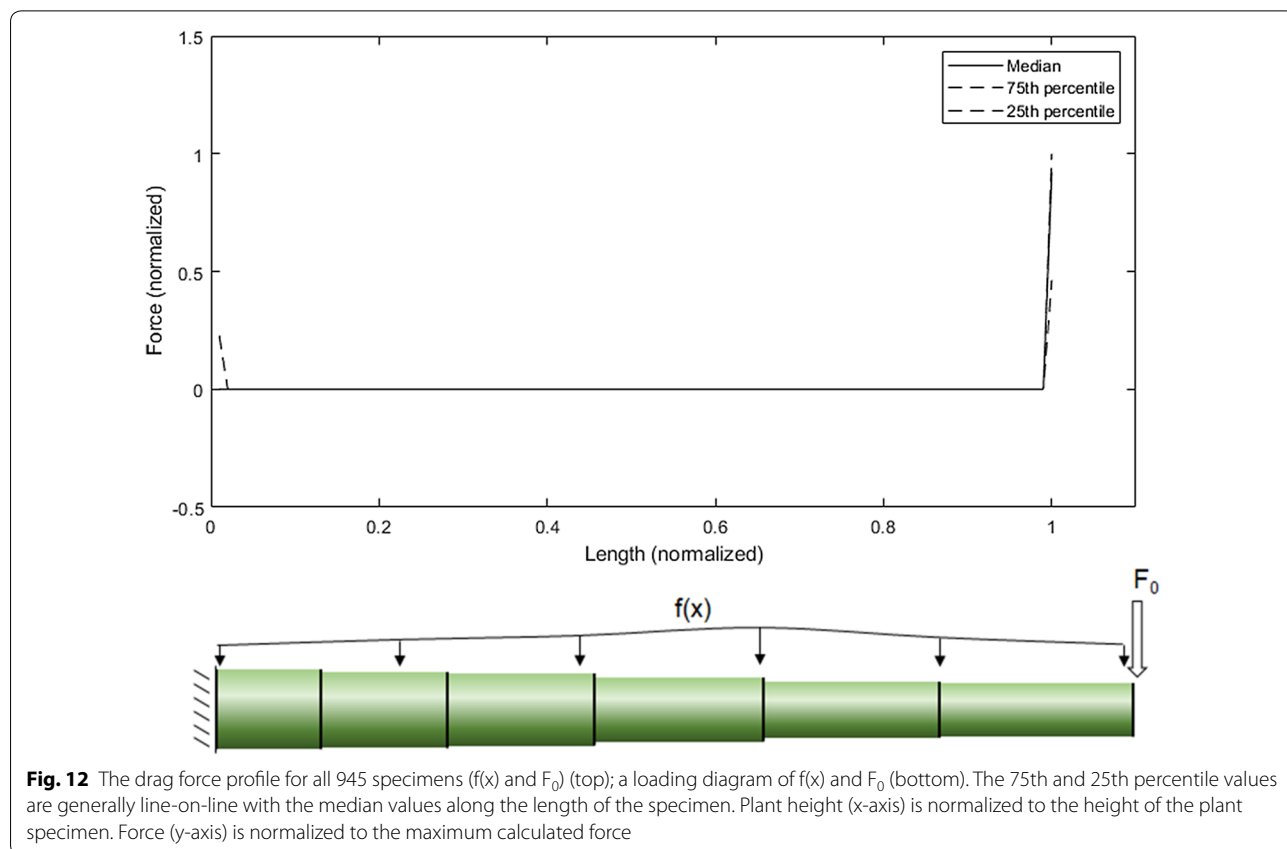
Page 13 of 15

Fig. 12). Thus these devices simulate the loading conditions experienced by plants in their natural environment and consequently produce natural failure types and patterns [8]. These devices are therefore expected to provide more distinguishing power than three-point-bending test methods.

This study elucidates the direct connection between stalk geometry (i.e., rind thickness and diameter) and stalk lodging resistance and demonstrates that key insights into stalk lodging resistance can be obtained through morphological phenotyping. However, most current morphological phenotyping tools require destructive sectioning and imaging procedures that induce plant fatality. These tools therefore prevent measurement of other important crop breeding metrics such as yield. Several nondestructive methods of measuring stalk geometry (i.e., rind thickness and diameter) have been developed (e.g., x-ray computed tomography) but these methods are usually limited to laboratory or greenhouse settings and cannot easily be implemented in an agricultural field setting (e.g., [23, 27, 29]). Future studies seeking to develop high throughput phenotyping methods capable of economically measuring internal and external stalk morphologies in the field are warranted and will lead to increased understanding of stalk lodging resistance.

Results showed that lodging resistant hybrids (i.e., those with higher average bending strengths) were more structurally efficient than hybrids that were weaker. The hybrids with higher average bending strengths also displayed less plant to plant variation in structural efficiency. In other words, strong hybrids were more structurally optimized and more consistently optimized than weaker plants (i.e., demonstrated less plant to plant variability). These same findings are true when analyzing individual plants. For example, if the hybrid factor is ignored and each stalk is analyzed as an individual specimen (i.e., no averaging of results across hybrids) the stronger stalks were more structurally efficient than weaker stalks. These results are likely due in part to breeding techniques used in the past. In particular, applied selective breeding pressure based on counts of lodged stalks at harvest time is expected to produce hybrids that are both strong and exhibit minimal plant to plant variance in strength. That is to say that a variety with high average strength but also high standard deviation in strength will have higher lodging rates than a variety with a similar average strength but a lower standard deviation in strength.

In this study, an optimization routine was used to determine the wind loading profile that would produce the most uniform mechanical stresses along the length of maize stalks. Based upon Fig. 12, which depicts the single resolved load (F_0) far exceeding the rest of the loading profile (f(x)), it was found that maize stalks are structurally optimized for wind loadings that occur primarily above the ear. This is consistent with the authors' observations in field conditions; although plants at the border of the field may experience loading along the full length of the stalk, the majority of maize plants appear to be primarily subjected to wind loads at or above the ear. The optimization method used in this study was robust and has the potential to be applied to other plants in which the structure of the plant may be predictive of its loading environment. Using optimization methods to infer a plants wind loading environment has several advantages over traditional measurement techniques used to determine wind loads on plants. In particular, it is computationally efficient (as compared to fluid–structure interaction models) and can infer the aggregate loading over time, taking into account the wind profile and fluid–structure interaction between the wind and the plant stalk.

Limitations

The primary limitation of the current study is that the rind of the stalk was assumed to be a homogeneous, isotropic, linear elastic material subjected to pure bending. The inclusion of heterogeneity, anisotropy, non-linear material properties, and the addition of the pith material could change the behavior of the analyzed stalks. However, previous research has shown the inclusion of these effects to be small and in many cases insignificant. The authors do not believe inclusion of such effects would change the overall conclusions of this paper [1, 37].

This study is deliberately limited in its scope to structural efficiency. Other abiotic and biotic considerations can affect stalk morphology/anatomy and should be considered in future studies [31]. In addition, this study utilized three-point-bending test to measure the bending strength of stem specimens. However, as mentioned previously these tests are less than ideal. Unfortunately, at the time the study was conducted by the authors we were not fully aware of the limitations of three-point-bending test. In particular, we did not expect to find that the majority of maize stalk cross-sections are structurally suboptimal. Future studies are warranted which utilize in-field phenotyping devices [12] to assess structural efficiency and its relations to stalk strength, harvest index, etc.

The assumption of the wind speed acting in the same direction along the length of the stalk is not necessarily valid [14], and as such was a key assumption made in this study. This assumption was used for this study, to avoid the trivial solution during the *fmincon* optimization routine, i.e., loading that frequently alternates directions to artificially reduce the residual values down

Stubbs *et al. Plant Methods*   (2020) 16:67

Page 14 of 15

to nearly zero in all cases. However, further improvements to the optimization parameters may yield more refined results in the future.

The modeling of maize stems as a structure comprised of a single homogeneous linear elastic orthotropic material is a simplifying assumption. Further analysis, including the inclusion of the pith material or the refinement of the model to incorporate the heterogeneous nature of the rind and pith tissue [35] would provide further insights into the structural efficiency of maize stems.

Conclusions

The morphology of physiological mature maize stalks was characterized, and the loading environments that result in the most uniform maximum stresses along the length of maize stalk were investigated. It was found that maize stalks are morphologically organized to resist wind loading that occurs primarily above the ear. It was also found that plants with higher bending strengths were more structurally efficient than weaker plants. However, even strong plants allocated structural tissues in a suboptimal manner. There exists much room for improvement in the area of structural optimization of maize stalks. These findings are relevant to crop management and breeding studies seeking to improve stalk lodging resistance.

Authors' contributions
All authors were fully involved in the study and preparation of the manuscript. All authors read and approved the final manuscript.

Availability of data and materials
The data sets obtained and analyzed during the current study are available from the corresponding author upon reasonable request.

Ethics approval and consent to participate
Not applicable.

Consent for publication
Not applicable.

Competing interests
The authors declare that they have no competing interest.

Author details
[1] Department of Mechanical Engineering, University of Idaho, 875 Perimeter Dr. MS0902, Moscow, ID 83844, USA. [2] School of Mathematical and Statistical Sciences, Clemson University, Clemson, SC 29634, USA. [3] Department of Genetics and Biochemistry, Clemson University, Biosystems Research Complex, Clemson, SC 29634, USA.

References
1. Al-Zube L, Sun W, Robertson D, Cook D. The elastic modulus for maize stems. Plant Methods. 2018;14:11.
2. Baker CJ. The development of a theoretical model for the windthrow of plants. J Theor Biol. 1995;175(3):355–72.
3. Baker CJ, Sterling M, Berry P. A generalized model of crop lodging. J Theor Biol. 2014;363:1–12.
4. Beer FP, Johnston E, Dewolf JT. Mechanics of materials. 3rd ed. New York: McGraw-Hill; 2002.
5. Berry PM, Spink JH, Gay AP, Craigon J. A comparison of root and stem lodging risks among winter wheat cultivars. J Agric Sci. 2003;141:191–202.
6. Berry P, Sylvester-Bradley R, Berry S. Ideotype design for lodging-resistant wheat. Euphytica. 2007;154:165–79.
7. Chuan W, Lei Y, Jianguo Z. Study on optimization of radiological worker allocation problem based on nonlinear programming function-fmincon. In: Proceedings of the 2014 IEEE international conference on mechatronics and automation. IEEE, 2014. p. 1073–1078.
8. Cook DD, de la Chapelle W, Lin T-C, Lee SY, Sun W, Robertson DJ. DARLING: a device for assessing resistance to lodging in grain crops. Plant Methods. 2019;15:102.
9. Cionco RM. A mathematical model for air flow in a vegetative canopy. J Appl Meteorol. 1965;4:517–22.
10. Dudley JW. Selection for rind puncture resistance in two maize populations. Crop Sci. 1994;34:1458–60.
11. Echezona BC. Corn-stalk lodging and borer damage as influenced by varying corn densities and planting geometry with soybean (Glycine max. L. Merrill). Int Agrophys. 2007;21:133–43.
12. Erndwein L, Cook D, Robertson D, Sparks E. Field-based mechanical phenotyping of cereal crops to assess lodging resistance. 2019. arXiv:1909.08555.
13. Esechie HA. Relationship of stalk morphology and chemical composition to lodging resistance in maize (*Zea mays* L.) in a rainforest zone. J Agric Sci. 1985;104:429–33.
14. Finnigan JJ. Turbulence in waving wheat. Bound Layer Met. 1978;16:181–211.
15. Finnigan J. Turbulence in plant canopies. Annu Rev Fluid Mech. 2000;32:519–71.
16. Flint-Garcia SA, Jampatong C, Darrah LL, McMullen MD. Quantitative trait locus analysis of stalk strength in four maize populations. Crop Sci. 2003;43:13–22.
17. Grafius JE, Brown HM. Lodging resistance in oats. Agron J. 1954;46:414–8.
18. Guo Q, Chen R, Ma L, Sun H, Weng M, Li S, Hu J. Classification of corn stalk lodging resistance using equivalent forces combined with SVD algorithm. Appl Sci. 2019;9:640.
19. Guo Q, Chen R, Sun X, Jiang M, Sun H, Wang S, Ma L, Yang Y, Hu J. A nondestructive and direction-insensitive method using a strain sensor and two single axis angle sensors for evaluating corn stalk lodging resistance. Sensors. 2018;18:1852.
20. Han SP. A globally convergent method for nonlinear programming. J Optim Theory Appl. 1977;22(3):297–309.
21. Heuschele DJ, Wiersma J, Reynolds L, Mangin A, Lawley Y, Marchetto P. The stalker: an open source force meter for rapid stalk strength phenotyping. HardwareX. 2019;6:e00067.
22. Holbert JR, Burlison WL, Biggar HH, Koehler B, Dungan GH, Jenkins MT. Early vigor of maize plants and yield of grain as influenced by the corn root, stalk, and ear rot diseases. J Agric Res. 1923;23:0583–630.
23. Mairhofer S, Zappala S, Tracy SR, Sturrock C, Bennett M, Mooney SJ, Pridmore T. RooTrak: automated recovery of three-dimensional plant root architecture in soil from X-ray microcomputed tomography images using visual tracking. Plant Physiol. 2012;158:561–9.
24. MATLAB. Find minimum of constrained nonlinear multivariable function—MATLAB. 2020. http://www.mathworks.com/help/optim/ug/fmincon.html.
25. Niklas KJ. Computing factors of safety against wind-induced tree stem damage. J Exp Bot. 2000;51:797–806.

Stubbs *et al. Plant Methods*   (2020) 16:67

Page 15 of 15

26. Niklas KJ, Spatz H. Methods for calculating factors of safety for plant stems. J Exp Biol. 1999;202:3273–80.
27. Robertson DJ, Julias M, Lee SY, Cook DD. Maize stalk lodging: morphological determinants of stalk strength. Crop Sci. 2017;57:926.
28. Robertson DJ, Smith SL, Cook DD. On measuring the bending strength of septate grass stems. Am J Bot. 2015;102:5–11.
29. Seegmiller WH, Graves J, Robertson DJ. A novel rind puncture technique to measure rind thickness and diameter in plant stalks. Plant Methods. 2020;16:44.
30. Sekhon R, Joyner C, Ackerman A, McMahan C, Cook D, Robertson D. Stalk bending strength is strongly associated with maize stalk lodging incidence across multiple environments. Field Crops Res. 2020;249:107737.
31. Sekhon R, Saski C, Kumar R, Flinn B, Luo F, Beissinger T, Ackerman A, Breitzman M, Bridges W, de Leon N, Kaeppler S. Integrated genome-scale analysis identifies novel genes and networks underlying senescence in maize. Plant Cell. 2019;31(9):1968–89.
32. Sreeraj P, Kannan T, Maji S. Prediction and optimization of weld bead geometry in gas metal arc welding process using RSM and fmincon. J Mech Eng Res. 2013;5(8):154–165.
33. Stubbs C, Baban N, Robertson D, Al-Zube L, Cook D. Bending stress in plant stems: models and assumptions. In: Geitmann A, Gril J, editors. Plant biomechanics—from structure to function at multiple scales. Berlin: Springer; 2018. p. 49–77.
34. Stubbs CJ, Larson R, Cook DD. Maize stem buckling failure is dominated by morphological factors. BioRxiv. 2019. p. 833863.
35. Stubbs CJ, Larson R, Cook DD. Mapping spatially distributed material properties in finite element models of plant tissue using computed tomography. 2020. bioRxiv.
36. Susko A. Deciphering lodging resistance in oat and other cereal crops. 2019.
37. Von Forell G, Robertson D, Lee SY, Cook DD. Preventing lodging in bioenergy crops: a biomechanical analysis of maize stalks suggests a new approach. J Exp Bot. 2015;66:4367–71.
38. Wen W, Gu S, Xiao B, Wang C, Wang J, Ma L, Wang Y, Lu X, Yu Z, Zhang Y. In situ evaluation of stalk lodging resistance for different maize (*Zea mays* L.) cultivars using a mobile wind machine. Plant Methods. 2019;15:1–16.
39. Yi C. Momentum transfer within canopies. J Appl Meteorol Climatol. 2008;47:262–75.
40. Young WC, Budynas RG. Roark's formulas for stress and strain. New York: McGraw-Hill; 2002.
41. Zienkiewicz O, Taylor R, Nithiarasu P. The finite element method for fluid dynamics. Amsterdam: Elsevier; 2014.

Publisher's Note